Int. J. Electrochem. Sci., 3 **(2008)** 199 - 215

International Journal of
ELECTROCHEMICAL
SCIENCE
www.electrochemsci.org

Chemical and Electrochemical (AC and DC) Studies on the Corrosion Inhibition of Low Carbon Steel in 1.0 M HCl Solution by Succinic Acid - Temperature Effect, Activation Energies and Thermodynamics of Adsorption

Mohammed A. Amin[*], *Sayed S. Abd El-Rehim, E.E. F. El-Sherbini, and Rady S. Bayoumi*

Chemistry Department, Faculty of Science, Ain Shams University, 11566 Abbassia, Cairo Egypt
[*]E-mail: maaismail@yahoo.com

Received: 4 November 2007 / *Accepted:* 29 November 2007 / *Online published:* 20 December 2007

The objective of this paper is to investigate the effect of temperature (15-65^{o}C) on the efficiency of succinic acid (SA), as an inhibitor, for the corrosion of a low cabon steel (LCS) electrode in aerated non-stirred 1.0 M HCl solutions (pH 4). Weight loss, potentiodynamic polarization and EIS (electrochemical impedance spectroscopy) techniques were applied to study the metal corrosion behaviour in the absence and presence of different concentrations of SA in this temperature range. Results obtained showed that the inhibition efficiency decreases with increase in temperature, indicating that SA physisorbs on the electrode surface. Activation energies have been calculated in the absence and presence of various concentrations of SA by measuring the temperature dependence of the corrosion rate obtained from the three methods. The adsorptive behaviour of SA on the LCS surface follows Temkin-type isotherm. The standard free energies of adsorption are lower than 40 kJ mol^{-1}, confirming the physisorption of SA on the electrode surface. Surface analysis using EDX (energy dispersive X-ray) confirmed the results obtained from chemical and electrochemical measurements. All the results obtained from the methods employed are in reasonable agreement.

Keywords: low carbon steel; HCl solution; Corrosion inhibition; succinic acid; impedance; physical adsorption, temperature effect

1. INTRODUCTION

Temperature has a great effect on the rate of metal electrochemical corrosion. In case of corrosion in a neutral solution, the increase of temperature has a favourable effect on the overpotential of oxygen depolarization and the rate of oxygen diffusion, but it leads to a decrease of oxygen solubility. In case of corrosion in an acid medium, the corrosion rate increases with temperature increase because the hydrogen evolution overpotential decreases.

Temperatures effects on acidic corrosion, most often in hydrochloric and sulphuric acids, have been the object of a large number of investigations [1–10]. It is generally assumed that in acid corrosion the inhibitors adsorb on the metal surface, resulting in a structural change of the double layer and reduced rate of the electrochemical partial reaction. Temperature dependence of the inhibitor efficiency (IE) and the comparison of the values of effective activation energy (E_a) of the corrosion process both in the absence and in the presence of inhibitors leads to some conclusions concerning the mechanism of the inhibiting action. Temperature increase leads to a decrease in IE, with the resulting variation of the effective activation energy value (the latter is, in general, higher than that in the inhibitor's absence) often interpreted as an indication of the formation of an adsorptive film of a physical (electrostatic) character. The opposite dependence (lower activation energy in an inhibited solution) demonstrates that a chemisorptive bond between the organic molecules and the metal surface is probable [1,8, 9, 11-13].

In our previous work [14], we investigated the efficiency of SA as a corrosion inhibitor for LCS in 1.0 M HCl solutions in the pH range (2-8), and we discussed the mechanism of adsorption. We have recently investigated the temperature dependence of the corrosion rate and obtained activation energy for the corrosion process of LCS in 1.0 M HCl solutions (pH 4) in the absence and presence of various concentrations of SA. It was also the purpose of the present work to test the experimental data with several adsorption isotherms at different temperatures, in order to determine the thermodynamic functions for the adsorption process and gain more information on the mode of adsorption of the inhibitor on the electrode surface.

These studies indicate that SA is physisorbed on the electrode surface. The results of these investigations are reported here. Chemical (weight loss) and electrochemical (polarization and impedance) measurements were used to obtain experimental data. Some EDX analysis were carried out.

2. EXPERIMENTAL PART

The working electrode employed in this work is made from LCS of composition presented in our previous study [14]. For weight loss measurements, corrosion inhibition tests were performed using rectangular coupons measuring 1x2x0.1 ml prepared from the LCS sheets. These coupons were first briefly ground with no. 600 emery paper, subsequently polished with no. 2000 emery paper, washed with deionized water, degreased with absolute ethanol, dried, and then rinsed with deionized water rapidly, followed by immediate rinsing with absolute ethanol.

The weight loss (in mg cm^{-2}) was determined at different immersion times and at different temperatures (15-65^{o}C) by weighing the cleaned samples before and after hanging the coupon into 100 ml of the corrosive solution, namely 1.0 M HCl (pH 4), (in open air) in the absence and presence of various concentrations of SA. After the time elapsed, the cleaning procedure consisted of wiping the coupons with a paper tissue and washing with distilled water and acetone, followed by oven drying at 125^{o}C. The pH 4 of 1.0 M HCl solution was adjusted by addition of NaOH. This pH value was

selected because it can be considered as a moderate point in the range of pH (2-8) that has been investigated in our previous study [14].

For electrochemical measurements, the investigated electrodes were cut as cylindrical rods, welded with Cu-wire for electrical connection and mounted into glass tubes of appropriate diameter using Araldite to offer an active flat disc shaped surface of (0.50 cm^2) geometric area, to contact the test solution. Prior to each experiment, the surface pre-treatment of the working electrode mentioned in weight loss measurements was performed.

A conventional electrochemical cell of capacity 100 ml was used containing three compartments for working, platinum spiral counter and reference electrodes. A Luggin-Haber capillary was also included in the design. The reference electrode was a normal calomel one used directly in contact with the working solution. The measurements were carried out in aerated non-stirred 1.0 M HCl solutions (pH 4) without and with various concentrations of SA at different temperatures (5-65^oC). All solutions were freshly prepared from analytical grade chemical reagents using doubly distilled water and were used without further purification. For each run, a freshly prepared solution, as well as a cleaned set of electrodes was used. Each run was carried out in aerated stagnant solutions at the required temperature ($\pm 1^oC$), using a water thermostat.

Electrochemical measurements were performed using A Potentiostat/Galvanostat (EG&G model 273) and lock-in amplifier (model 5210) connected with a personal computer. Various electrochemical parameters were simultaneously determined using M352 corrosion software and M398 impedance software from EG&G Princeton Applied Research. The potentiodynamic current-potential curves were carried out at a scan rate of 0.10 mV s^{-1}. Impedance measurements were carried out using AC signals of amplitude 5 mV peak to peak at the open circuit potential in the frequency range 30 kHz to 1.0 mHz. All impedance data were fitted to appropriate equivalent circuits using the computer program EQUIVCRT [15]. Before polarization and impedance experiments, the open circuit potential of the working electrode was measured as a function of time during 60 min, the time necessary to reach a quasi-stationary value for the open circuit potential at the specified conditions.

The composition of the corrosion products formed on the surface of LCS immersed for 60 min in 1.0 M HCl solutions (pH 4) containing 0.001 M SA were analyzed at different temperatures by means of EDX using a Traktor TN-2000 energy dispersive spectrometer. The LCS samples were finally washed thoroughly and submitted to 5 min of ultrasonic cleaning in order to remove loosely adsorbed ions.

3. RESULTS AND DISCUSSION

3.1. Chemical methods

3.1.1. Weight loss measurements

The effect of temperature on the inhibited acid-metal reaction is highly complex, because many changes occur on the metal surface, such as rapid etching and desorption of the inhibitor and the inhibitor itself, in some cases, may undergo decomposition and/or rearrangement. In the present work,

the rate of the corrosion process with the temperature increase was studied in 1.0 M HCl solutions (pH 4) both in the absence and in the presence of various concentrations of SA. Figure 1, as an example, shows the effect of temperature (15-65^{o}C) on the variation of the weight loss (in mg cm^{-2}) of a LCS electrode with the immersion time in 1.0 M HCl solution (pH 4) containing 0.001 M SA. Similar results were obtained for other concentrations of SA. The slope of each line (weight loss per unit time; mg cm^{-2} h^{-1}) represents the corrosion rate of LCS at the specified conditions. It follows from the data of Fig. 1 that the weight loss (and hence the rate of corrosion) increased, and therefore the corrosion inhibition decreased, with increase in temperature.

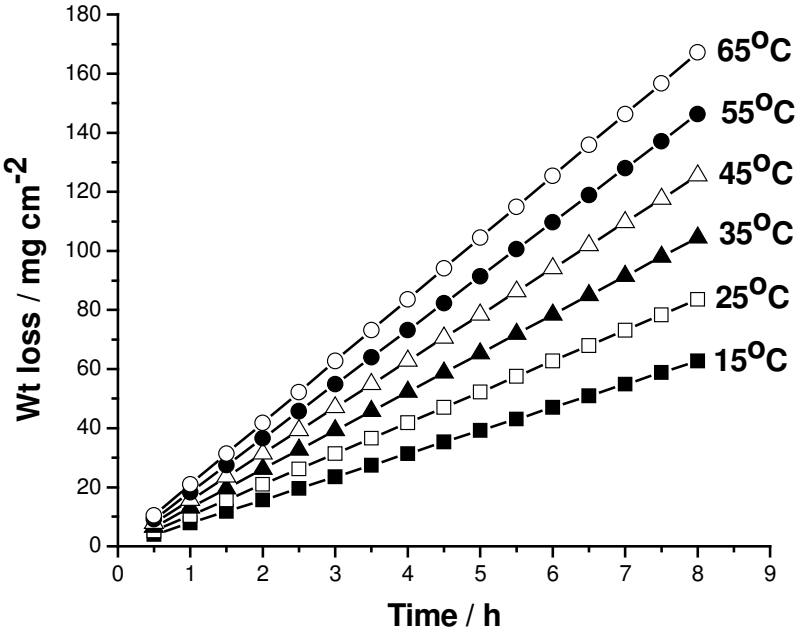

Figure 1. Variation of the weight loss data (in mg cm^{-2}) with the immersion time recorded for a LCS electrode in 1.0 M HCl solution (pH 4) containing 0.001 M SA at different temperatures (15-65^{o}C).

The inhibition efficiency (IE%) values were calculated for LCS in 1.0 M HCl solutions (pH 4) containing various concentrations (0.0001–0.10 M) of SA at different temperatures, using equation (1) [16-18]:

$$IE\% = [1 - (WL / WL^{o})] \times 100 \quad (1)$$

where WL^{o} and WL are the weight losses of speciemens without and with inhibitor. Figure 2 shows the dependence of inhibitor efficiency on temperature when different amounts of inhibitor are added. The plots in Fig. 2 have S-shaped adsorption isotherms, indicating that inhibition takes place through adsorption of SA on the electrode surface [16-18]. Our previous study showed that the inhibitor is electrostatically adsorbed on the electrode surface [14]. At a given temperature, the inhibition efficiency increases with increasing SA concentration, since more succinate anions will electrostatically adsorbed on the electrode surface [14]. It is seen that SA has inhibiting properties at

all the studied temperatures and the values of IE% decrease with temperature increase. This shows that the inhibitor has experienced a significant decrease in its protective properties with increase in temperature. This decrease in the protective properties of the inhibitor with increase in temperature may be connected with two effects; a certain drawing of the adsrption-desorption equilibrium towards desorption (meaning that the strength of adsorption process decreases at higher temperatures) and roughening of the metal surface which results from enhanced corrosion. These results suggest that physical adsorption may be the type of adsorption of the inhibitor on the LCS surface.

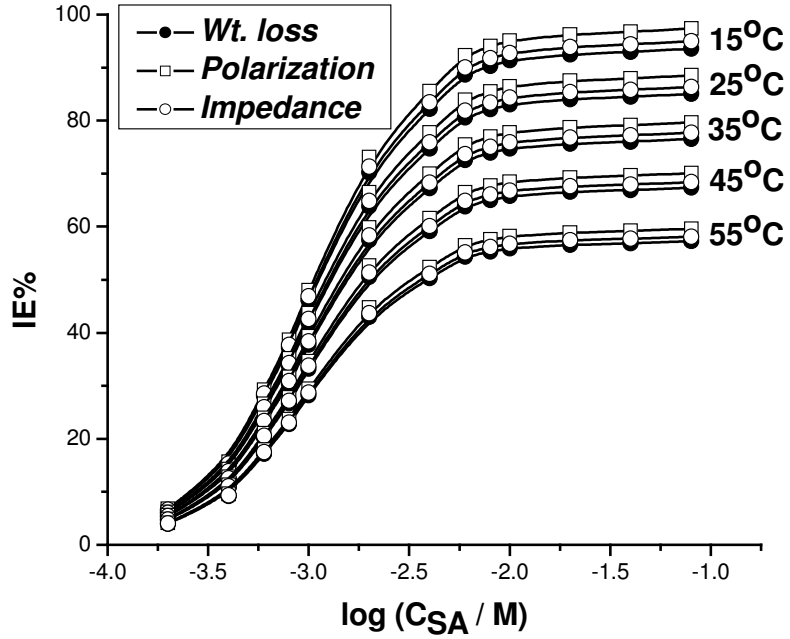

Figure 2. Dependence of the inhibition efficiency (IE%), calculated from the weight loss, polarization and impedance data, on the logarithmic concentration of the inhibitor (log C_{inhib}) for a LCS electrode in 1.0 M HCl solution (pH 4) at different temperatures (15-65^{o}C).

3.2. Electrochemical methods

3.2.1. Polarization measurements

In this section, we were interested in exploring the activation energy of the corrosion process and the thermodynamics of adsorption of SA (as will be discussed later in section 3.5.). This was accomplished by investigating the temperature and concenration dependences of the corrosion current obatined using the Tafel extrapolation method. These measurements were done in the poential region ± 200 mV from the corrosion potential (E_{corr}) at a sweep rate of 0.10 mV s^{-1}. The corrosion potential was obtained by measuring the open circuit potential as a function of time [14]. The corrosion current density (j_{corr}) was determined by extrapolating the Tafel lines.

Figure 3 illustrates the effect of temperature (15-65 ^{o}C) on the Tafel plots recorded for LCS electrode in 1.0 M HCl solution (pH 4) with the addition of 0.001 M SA. Analogous Tafel plots were obtained for other concentrations of SA over the same temperature range. It is obvious from Fig. 3 that

the corrosion potential (E_{corr}) shifts towards more negative values and both anodic and cathodic current densities of LCS corrosion were enhanced upon increasing temperature.

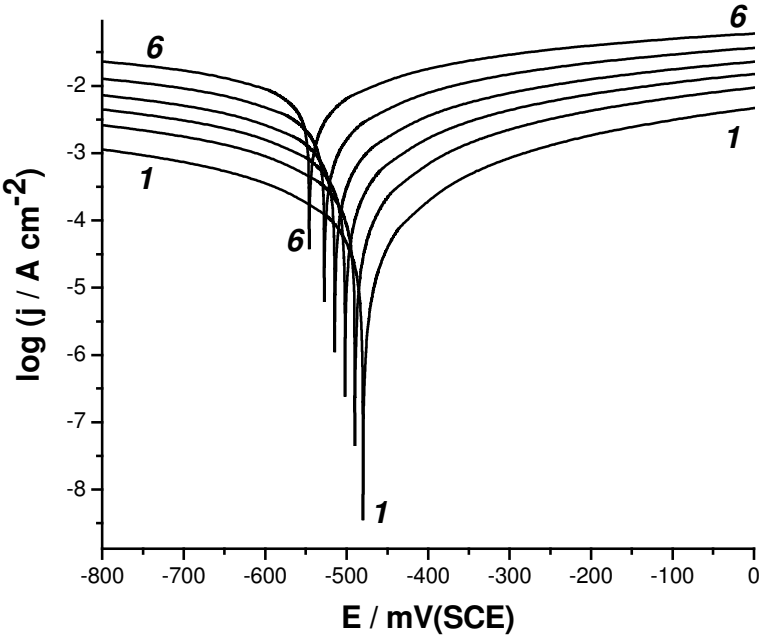

Figure 3. Effect of temperature (15-65°C) on the potentiodynamic anodic and cathodic polarization characteristics of a LCS electrode in 1.0 M HCl solution (pH 4) containing 0.001 M SA at a scan rate of 0.10 mV s^{-1}. (1) 15 °C; (2) 25 °C; (3) 35 °C; (4) 45 °C; (5) 55 °C; (6) 65 °C.

The electrochemical parameters, such as corrosion potential (E_{corr}), cathodic and anodic Tafel slopes (b_c and b_a), corrosion current density (j_{corr}) and the polarization resistance (R_p) were recorded for LCS in 1.0 M HCl solutions (pH 4) without and with 0.001 M SA at different temperatures. Table 1, as an example, collects these electrochemical parameters at 25°C. As can be seen from these polarization results, the j_{corr} values increase, and therefore the rate of corrosion is enhanced, with increase in temperature.

Table 1. The electrochemical parameters ($j_{corr.}$, $E_{corr.}$, b_c and b_a and R_p) associated with polarization measurements of LCS electrode in 1.0 M HCl solution (pH 4) containing 0.001 M SA at different temperatures.

T / K	j_{corr} / mA cm^{-2}	E_{corr} / V(SCE)	b_a / V $dec.^{-1}$	b_c / V $dec.^{-1}$	R_p / kΩ
288	0.11	-480.00	196.00	165.00	45.97
298	0.23	-490.00	196.00	166.00	36.67
308	0.40	-502.00	195.00	164.00	25.92
318	0.89	-516.00	194.00	166.00	17.98
328	2.34	-527.00	195.00	165.00	10.25
338	5.50	-549.00	196.00	166.00	5.00

The j_{corr} values were used to calculate IE% values of SA in 1.0 M HCl solutions (pH 4) as a function of SA concentration and temperature (see Fig. 2), using equation (2) [18].

$$IE\% = 100 \times [(j^{o}_{corr} - j_{corr}) / j^{o}_{corr}] \quad (2)$$

where j^{o}_{corr} and j_{corr} are the corrosion current densities for uninhibited and inhibited solutions, respectively. The inhibition efficiency increases with increase in SA concentration, while it decreases with increase in temperature, confirming the occurrence of physical adsorption.

3.2.2. Impedance measurements

In this study, complex plane impedance plots were recorded for LCS in 1.0 M HCl solutions (pH 4) in the temperature range (15-65^{o}C) without and with various concentrations of SA at the respective open circuit potentials. Figure 4, as an example, shows the effect of temperature on the impedance response of LCS in 1.0 M HCl solution (pH 4) containing 0.001 M SA at the respective open circuit potentials. It clear from Fig. 4 that at all temperatures, the impedance spectra are characterized by a depressed charge-transfer semicircle at high frequencies (HF) followed by an inductive loop in the low-frequency (LF) values. The HF semicircle was attributed to the time constant of charge transfer and double-layer capacitance [14,19-21] and the LF inductive loop to the relaxation process obtained by adsorption species as $Cl^{-}_{ads.}$ and $H^{+}_{ads.}$ on the electrode surface [22]. The equivalent circuit used to fit the experimental data and extract the impedance parameters (R_{ct} and C_{dl}) which characterize the corrosion process is present elsewhere [14].

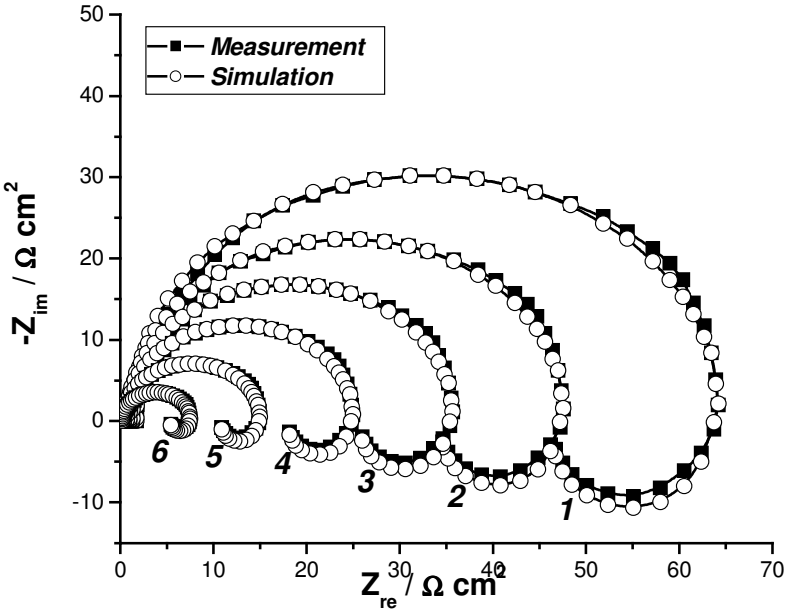

Figure 4. Complex plane impedance plots recorded for a LCS electrode in 1.0 M HCl solution (pH 4) containing 0.001 M SA at diffferent temperatures (15-65 ^{o}C) and at the respective open circuit potentials. (1) 15 ^{o}C; (2) 25 ^{o}C; (3) 35 ^{o}C; (4) 45 ^{o}C; (5) 55 ^{o}C; (6) 65 ^{o}C.

The impedance parameters have been calculated at different temperatures and listed in Table 2. Inspection of the data of Table 2 reveals that the temperature increase leads to an essential decrease of R_{ct} and an increase of C_{dl} values which on one hand may be attributed to the corrosion rate increase and on the other hand to the probable partial desorption of the inhibitor under these conditions. But the concentration of the inhibitor is high to sustain an inhibiting adsorption layer at a given temperature. It may be assumed that the density of the inhibitor adsorbed layer within outer Helmholtz layer (OHL) decreases, while the diffuse part of the double electrical layer increases with temperature. This effect is accompanied by a certain decrease in the depression of the adsorption capacitive semicircle (see Fig. 4).

Table 2. Values of "K" and "a" recorded for LCS electrode in 1.0 M HCl solution (pH 4) containing 0.001 M SA obtained by applying Temkin isotherm on the weight loss, polarization and impedance data at different temperatures.

T / K	**K**			**a**		
	Wt. loss	**Polarization**	**Impedance**	**Wt loss**	**Polarization**	**Impedance**
288	10969	11035	10550	0.10	0.11	0.09
298	10210	10750	10150	0.09	0.10	0.08
308	9250	10250	9025	0.08	0.085	0.075
318	8155	8250	8110	0.07	0.075	0.06
328	6950	7100	6895	0.06	0.07	0.055
338	5900	6030	5875	0.045	0.05	0.035

The R_{ct} values were used to calculate the IE% of SA at different concentrations and temperatures (see Fig. 2), using equation 3 [18].

$$IE\% = 100 \times [(R_{ct} - R^{o}_{ct}) / R_{ct}] \quad (3)$$

where R_{ct}^{o} and R_{ct} are the charge transfer resistances for uninhibited and inhibited solutions, respectively. It is apparent that the inhibition efficiency increases with increasing inhibitor concentration, while it decreases with increasing temperature, confirming the suggestion that physical adsorption occurs. It is worth noting from Fig. 2 that the inhibition efficiencies obtained from impedance measurements are comparable and run parallel with those obtained from weight loss and potentiodynamic polarization methods.

3.3. EDX examinations of the electrode surface

In our previous study [14], EDX survey spectra showed that a carbonaceous material containing oxygen atoms (due to the adsorption of SA) has covered the electrode surface. The amount of SA adsorbed increases with increasing inhibitor concentration, pH and immersion time, as evidenced from the high contribution of carbon and oxygen signals. In this section, we are interested in studying the effect of temperature on the EDX spectra of LCS samples immersed for 60 min in 1.0 M

HCl solution (pH 4) containing 0.001 M SA (see Fig. 5). The aim of this section is to confirm the results obtained from chemical and electrochemical measurements that SA is physically adsorbed on

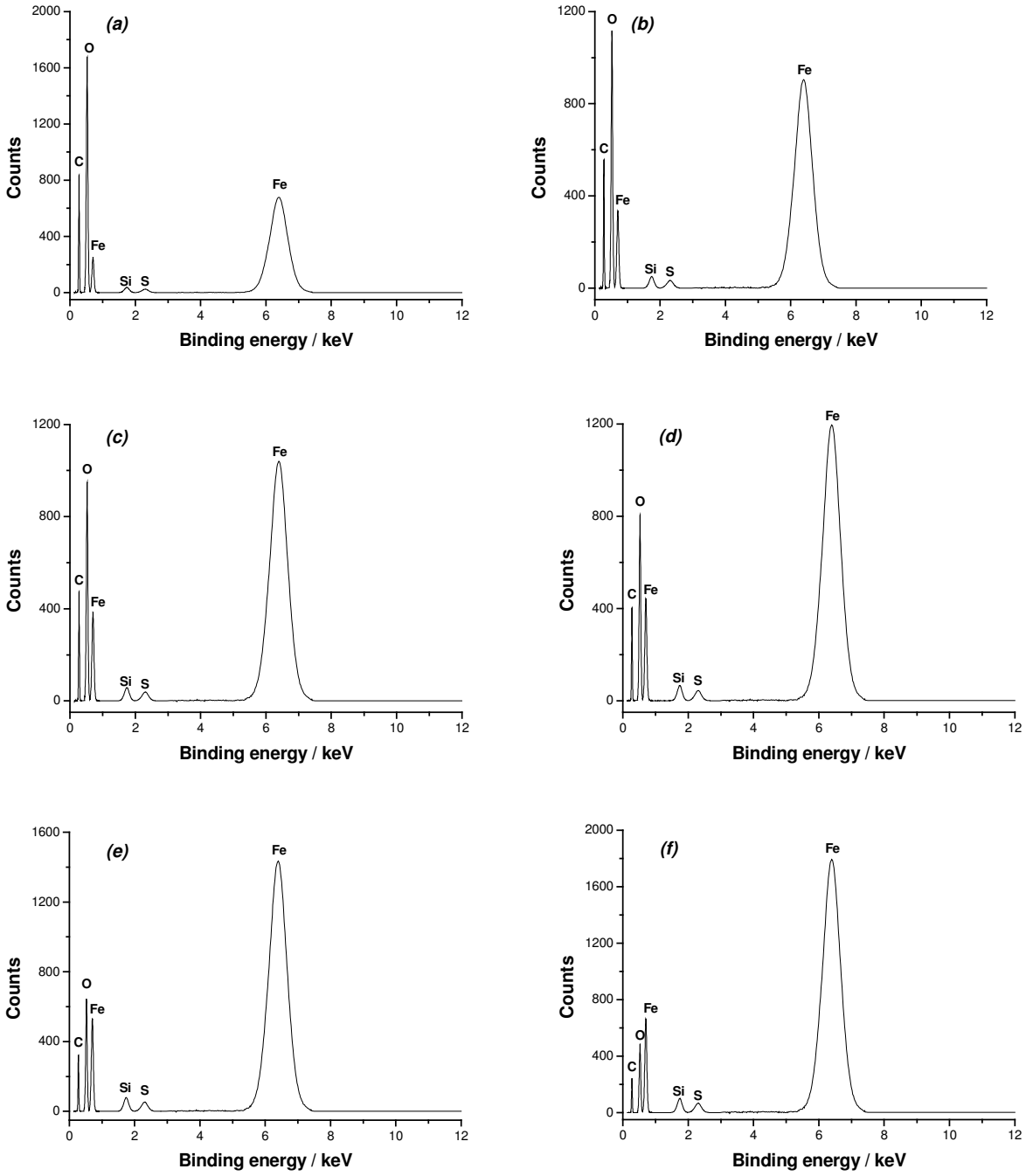

Figure 5. effect of temperature (15-65^{o}C) on the EDX spectra recorded for LCS samples immersed for 60 min in 1.0 M HCl solution (pH 4) containing 0.001 M SA (a) 15 ^{o}C; (b) 25 ^{o}C; (c) 35 ^{o}C; (d) 45 ^{o}C; (e) 55 ^{o}C; (f) 65 ^{o}C.

the electrode surface. It is obvious from Fig. 5 that the carbon and oxygen signals are considerably suppressed and that of Fe are significantly enhanced with increasing temperature (see Fig. 5 a-f). This

suppression in carbon and oxygen signals and the enhancement in Fe signals with increasing temperature indicates that the inhibitor's efficiency is reduced due to its desorption from the metal surface and enhancement of the metal corrosion process. These results confirm the occurrence of physical adsorption.

3.4. Adsorption isotherms and thermodynamic functions of the adsorption process

The values of surface coverage (θ = IE% / 100) to different concentrations of SA, obtained from weight loss, polarization and impedance measurements in the range of temperature (15-65°C), have been used to explain the best isotherm to determine the adsorption process. The LCS corrosion inhibition by SA can be explained by the adsorption of SA on the LCS surface so as to impede the electron transfer. The adsorption of inhibitor molecules from aqueous solutions can be regarded as a quasi-substitution process between the organic compound in the aqueous phase $Org_{(aq.)}$ and water molecules at the electrode surface, $H_2O_{(s)}$

$$Org_{(aq.)} + x\ H_2O_{(s)} = Org_{(s)} + x\ H_2O \qquad (4)$$

where x, the size factor, is the number of water molecules displaced by one molecule of organic inhibitor. Adsorption isotherms are very important in determining the mechanism of organo-electrochemical reactions [23]. The most frequently used isotherms are Langmiur, Frumkin, Hill de Boer, Parsons, Temkin, Flory-Huggins and Dahar-Flory-Huggins and Bockris-Swinkel [24-32]. All these isotherms are of the general form:

$$f(\theta,x)\exp(2a\theta) = KC \qquad (5)$$

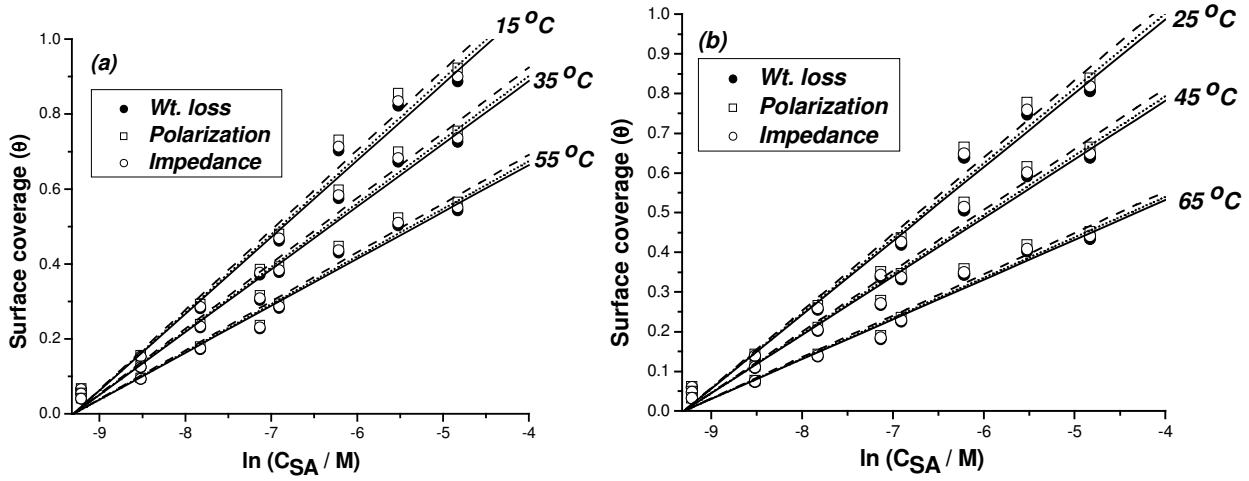

Figure 6. Curve fitting of weight loss, polarization and impedance data obtained for a LCS electrode in 1.0 M HCl solution (pH 4) containing 0.001 M SA to Temkin adsorption isotherm at different temperatures. (a) 15 °C, 35 °C and 55 °C (b) 25 °C, 45 °C and 65 °C

where f (θ,x) is the configurational factor which depends upon the physical model and the assumptions underlying the derivation of the isotherm, θ the surface coverage degree, C the inhibitor concentration in the bulk of solution, "a" the lateral interaction term describing the molecular interactions in the adsorption layer and the heterogeneity of the surface and is a measure for the steepness of the adsorption isotherm. K the adsorption-desorption equilibrium constant.

In the range of temperature studied, the best correlation between the experimental results, obtained from the three techniques, and the isotherm functions was obtained using Temkin adsorption isotherm (Equation 6).

$$\exp(2a\theta) = KC \quad (6)$$

Figure 6 (a and b) represents fitting of weight loss, polarization and impedance data obtained for LCS electrode in 1.0 M HCl solution (pH 4) containing 0.001 M SA to Temkin isotherm at different temperatures (15 ^{o}C-65 ^{o}C). The isotherms' parameters (K and a) and the free energies of the inhibitor adsorption calculated from the equation [33]:

$$K = (1/55.5) \exp(-\Delta G^{o}_{ads}/RT) \quad (7)$$

are shown in Tables 2 and 3, respectively. ΔG^{o}_{ads} is the free energy of adsorption, 55.5 the concentration of water in the solution in mol l^{-1}, R the universal gas constant, T the thermodynamic temperature. It follows from the theory of adsorption from solutions [33] that:

$$(d \ln K/dT)_{\theta} = - \Delta H^{o}_{ads}/RT^{2} \quad (8)$$

Where ΔH^{o}_{ads} is the isosteric enthalpy of adsorption. The integrated version of the Vant Hoff equation:

$$\ln K = - \Delta H^{o}_{ads}/RT + \text{constant} \quad (9)$$

may be used to determine ΔH^{o}_{ads}. The slopes of the lines, shown in Fig. 7, depict the linear relation between lnK and (1/T) at a given surface coverage. These slopes, multiplied by R, give the values of ΔH^{o}_{ads} shown in Table 3. The values of the entropy change of the inhibitor adsorption (ΔS^{o}_{ads}), listed in Table 3, was calculated from the equation [18]:

$$\Delta G^{o}_{ads} = \Delta H^{o}_{ads} - T \Delta S^{o}_{ads} \quad (10)$$

It follows from the data of Table 3 that there is a good agreement between the values of K obtained from the three techniques. The values of K are relatively low and decrease with an increase in temperature. Large values of K mean better inhibition efficiency of the inhibitor, i.e., strong electrical interaction between the double layer existing at the phase boundary and the adsorbing inhibitor molecules. Small values of K, however compromise that such interactions between adsorbing inhibitor

molecules and the metal surface are weaker, indicating that the inhibitor molecules are easily removable by the solvent molecules from the surface. These results confirm the suggestion that this inhibitor is physically adsorbed on the metal surface and the strength of the adsorption decreases with temperature. Small and positive values of "a" would indicate the existence of weak lateral forces of attraction between adsorbate molecules in the adsorption layer [33].

Table 3. The thermodynamic parameters of adsorption process obtained from the weight loss, polarization and impedance data by applying Temkin isotherm for LCS electrode in 1.0 M HCl solution (pH 4) containing various concentrations of SA at 25°C.

C_{inhib} / M	Wt. Loss			Polarization			Impedance		
	ΔH^o_{ads}/ kJ mol^{-1}	ΔG^o_{ads}/ kJ mol^{-1}	ΔS^o_{ads}/ J mol^{-1} K^{-1}	ΔH^o_{ads}/ kJ mol^{-1}	ΔG^o_{ads}/ kJ mol^{-1}	ΔS^o_{ads}/ J mol^{-1} K^{-1}	ΔH^o_{ads}/ kJ mol^{-1}	ΔG^o_{ads}/ kJ mol^{-1}	ΔS^o_{ads}/ J mol^{-1} K^{-1}
0.0001	-3.28	-25.12	73.38	-3.41	-26.00	75.90	-3.20	-24.49	71.53
0.0002	-4.75	-26.15	71.90	-4.94	-27.07	74.36	-4.63	-25.50	70.12
0.0004	-6.50	-27.50	70.56	-6.76	-28.46	72.91	-6.34	-26.81	68.78
0.0008	-9.20	-29.25	67.37	-9.57	-30.27	69.55	-8.97	-28.52	65.69
0.0010	-10.50	-30.00	65.52	-10.92	-31.05	67.64	-10.24	-29.25	63.87
0.0020	-13.44	-32.00	62.36	-13.98	-33.12	64.31	-13.10	-31.20	60.82
0.0040	-15.74	-33.50	59.67	-16.37	-34.67	61.49	-15.35	-32.66	58.16
0.0080	-20.69	-35.99	51.41	-21.52	-37.25	52.85	-20.17	-35.09	50.13
0.0100	-24.69	-37.10	41.70	-25.68	-38.40	42.74	-24.07	-36.17	40.66
0.0200	-25.33	-37.25	40.05	-26.34	-38.55	41.03	-24.70	-36.32	39.04
0.0400	-25.45	-37.40	40.15	-26.47	-38.71	41.13	-24.81	-36.47	39.18
0.0800	-25.61	-37.42	39.68	-26.63	-38.73	40.66	-24.97	-36.48	38.67
0.1000	-25.87	-37.44	38.88	-26.90	-38.75	39.82	-25.22	-36.50	37.90

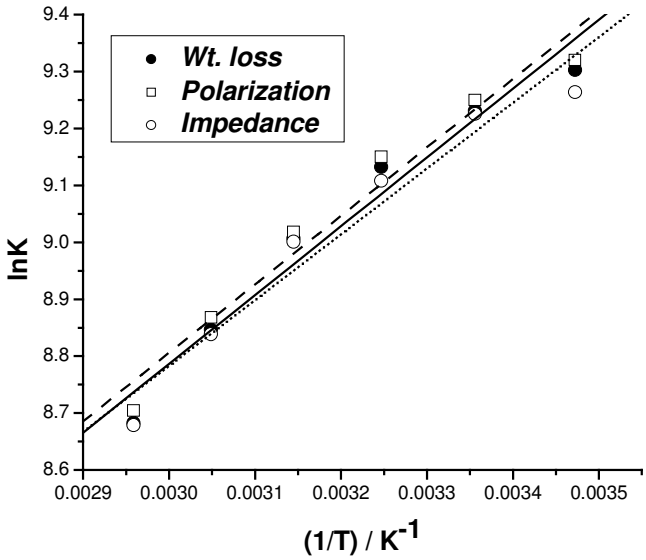

Figure 7. Relation between log (binding constant) and 1/T for a LCS electrode in 1.0 M HCl solution (pH 4) containing 0.001 M SA obtained by applying Temkin adsorption isotherm on weight loss, polarization and EIS data.

The negative values of ΔG^{o}_{ads} ensure the spontaneity of the adsorption process and stability of the adsorbed layer on the electrode surface. Generally, values of ΔG^{o}_{ads} lower than –40 kJ mol^{-1} are consistent with the electrostatic interaction between the charged molecules and the charged metal (physisorption); those around –50 kJ mol^{-1} or higher involve charge shairing or charge transfer from organic molecules to the metal surface to form a coordinate type of bond (chemisorption) [32,34]. In the present work, the calculated values of ΔG^{o}_{ads} are lower than –40 kJ mol^{-1}, indicating, therefore, that the adsorption mechanism of SA on LCS surface in 1.0 M HCl solutions (pH 4) was typical of physisorption (see Table 3).

The negativity of the enthalpy (Table 3) means that heat is released from the adsorption process. Generally, an exothermic adsorption process signifies either physi- or chemi-sorption, while endothermic process is attributable unequivocally to chemi-sorption [35]. In an exothermic process, physi-sorption is distinguished from chemi-sorption by considering the absolute value of adsorption enthalpy. Typically, the enthalpy of a physi-sorption process is lower than 41.86 kJ mol^{-1}, while that of a chemi-sorption process approaches 100 kJ mol^{-1} [35,36].

In the present work, the absolute values of enthalpy are low approaching those typical of physi-sorption (see Table 3). The absolute value of the adsorption enthalpy, $|\Delta H^{o}_{ads}|$, increases with the increase in surface coverage due to the attractive interaction between the adsorbed molecules indicating the validity of the Temkin model [33]. The origin of the attractive forces is most probably the dipole-dipole interaction occurring between the neighbouring adsorbed molecules [37].

Table 3 clearly shows that the values of ΔS^{o}_{ads} decrease with increasing inhibitor concentration. The entropy changes can be explained in terms of displacement of the H_2O molecules from the surface into the hydrogen-bonded aqueous solution and adsorption of inhibitor molecules at the surface from their surface-active positions in the solution phase [38].

3.5. Thermodynamic activation functions of the corrosion process

Further insight into the adsorption mechanism is offered by considering the thermodynamic functions for the LCS dissolution in HCl solutions in the absence and presence of various concentrations of the inhibitor. These thermodynamic functions were obtained by applying the Arrhenius and the transition-state equations [39].

$$\ln (\text{rate}) = - (E_a^{o} / RT) + \text{constant} \quad (11)$$

$$\text{rate} = (RT/Nh) \exp (\Delta S^{o}_{a} / R) \exp (-\Delta H^{o}_{a} / RT) \quad (12)$$

where E_a^{o} is the apparent activation energy, ΔS^{o}_{a} the apparent entropy of activation, ΔH^{o}_{a} the apparent enthalpy of activation, h Plank's constant, and N the Avogadro's number. Since the values of surface coverage (θ = IE% / 100) were taken as a measure of the efficiency of the inhibitor. This is evident from the increase of θ (i.e., high inhibition efficiency) with increase in inhibitor concentration, and its decrease with increase in temperature (i.e., low inhibition efficiency due to the physisorption of SA on the electrode surface), as shown in Fig. 2. Hence the values of (1-θ) may be considered as a direct

measure of the corrosion rate. The values of (1-θ) to different concentrations of SA, obtained from weight loss, polarization and impedance measurements, in the range of temperature (15-65°C) have, therefore, been used to calculate the rate of corrosion in equations 11 and 12.

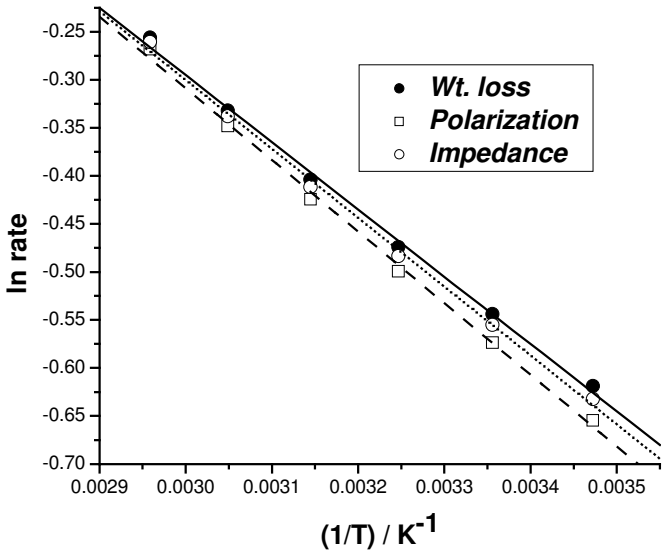

Figure 8. Arrhenius plot of the corrosion rate, obtained from weight loss, polarization and impedance data, recorded for a LCS electrode in 1.0 M HCl solution (pH 4) containing 0.001 M SA.

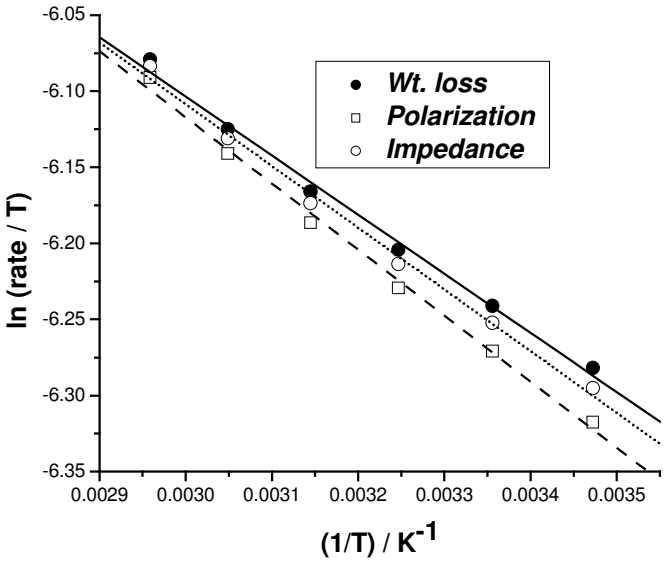

Figure 9. Transition State plot of the corrosion rate, obtained from weight loss, polarization and impedance data, recorded for a LCS electrode in 1.0 M HCl solution (pH 4) containing 0.001 M SA.

Arrhenius and Transition state plots obtained from weight loss, polarization and impedance measurements, were constructed for LCS in 1.0 M HCl solution (pH 4) containing various

concentrations of SA in the range of temperature (15-65°C). Figures 8 and 9 represent, respectively, Arrhenius and Transition state plots, obtained from the three methods, of LCS in 1.0 M HCl solution (pH 4) containing 0.001 M SA (as an example). The values of these thermodynamic activation functions were calculated from Arrhenius and Transition state plots and listed in Table 4. The decrease of IE% values with temperature increase (Fig. 2) and the higher values of E_a^o in presence of SA than in its absence (Table 4) can be interpreted as an indication of physi-sorption. In general, the proceeding of physical adsorption requires the presence of both electrically charged metal surface and charged species in the bulk of the solution. This point has been discussed in details in our previous study [14].

Table 4. The thermodynamic activation parameters of the metal dissolution process obtained from the weight loss, polarization and impedance data by applying Arrhenius and Transition State plots for LCS electrode in 1.0 M HCl solution (pH 4) containing various concentrations of SA.

C_{inhib} / M	Wt. Loss			Polarization			Impedance		
	E^o_a / kJ mol^{-1}	ΔH^o_a / kJ mol^{-1}	ΔS^o_a / J mol^{-1} K^{-1}	E^o_a / kJ mol^{-1}	ΔH^o_a / kJ mol^{-1}	ΔS^o_a / J mol^{-1} K^{-1}	E^o_a / kJ mol^{-1}	ΔH^o_a / kJ mol^{-1}	ΔS^o_a / J mol^{-1} K^{-1}
Blank									
0.0001	3.88	2.00	-210	3.93	2.03	-212	3.85	1.97	-208
0.0002	4.12	2.12	-216	4.17	2.16	-218	4.09	2.10	-214
0.0004	4.90	2.45	-221	4.96	2.49	-223	4.86	2.42	-218
0.0008	5.85	2.98	-228	5.93	3.03	-230	5.81	2.94	-225
0.0010	6.24	3.55	-239	6.32	3.61	-241	6.19	3.50	-236
0.0020	10.75	5.80	-255	10.89	5.90	-257	10.67	5.72	-252
0.0040	17.55	8.44	-270	17.78	8.58	-272	17.42	8.32	-267
0.0080	22.27	11.00	-284	22.56	11.19	-286	22.11	10.85	-280
0.0100	25.15	15.25	-298	25.48	15.51	-300	24.97	15.04	-294
0.0200	25.22	15.33	-300	25.55	15.59	-302	25.04	15.12	-296
0.0400	25.28	15.36	-302	25.61	15.62	-304	25.10	15.15	-298
0.0800	25.30	15.40	-305	25.63	15.66	-307	25.12	15.19	-301
0.1000	25.32	15.42	-308	25.65	15.68	-310	25.14	15.21	-304

The increase in E_a^o is proportional to the inhibitor concentration, indicating that the energy barrier for the corrosion interaction is also increased [40-42]. This means that the corrosion reaction will be further pushed to the surface sights that are characterised by progressively higher values of E_a^o as the concentration of the inhibitor in the solution becomes larger. In other words, the adsorption of the inhibitor on the electrode surface leads to the formation of a physical barrier that reduces the metal reactivity in the electrochemical reactions of corrosion [43]. The positive sign of the enthalpy reflects the endothermic nature of the LCS dissolution process.

Large and negative values of the entropy imply that the activated complex in the rate determining step represents an association rather than a dissociation step, meaning that a decrease in disordering takes place on going from reactants to the activated complex [16,17].

4. CONCLUSIONS

In this work, chemical (weight loss) and electrochemical (polarization and impedance) methods were used to study the effect of temperature (15-65 ^{o}C) on the ability of SA to inhibit the corrosion of LCS in aerated stagnant 1.0 M HCl solutions (pH 4). The principle conclusions are:

- The chemical and electrochemical investigations showed that the rate of corrosion on the LCS surface free from the inhibitor (SA) decreases, as well as the protective action of the adsorbed inhibitor layer decreases with temperature increase.
- The thermodynamic parameters revealed that the inhibition of corrosion by SA is due to the formation of a physisorbed film of the inhibitor on the metal surface.
- Adsorption of SA was found to follow Temkin adsorption isotherm.
- The inhibition efficiency (IE%) of SA was temperature-dependent and its addition led to an increase of the activation corrosion energy.
- EDX spectra recorded for LCS samples, immersed in 1.0 M HCl solutions (pH 4) containing 0.001 M SA at different temperatures, confirmed the results obtained from chemical and electrochemical methods that SA is physisorbed on the electrode surface.
- The results obtained from weight loss, dc polarization and ac impedance are in reasonably good agreement.

References

1. N.P. Zhuk, Course on Corrosion and Metal Protection, Metallurgy, Moscow, 1976.
2. G. Perboni and G. Rocchini, Proceedings of the 10th ICMC, Madras, India, 1988, p. 2763.
3. I.H. Omar, G. Trabanelli and F. Zucchi, Proceedings of the 10th ICMC, Madras, India, 1988, p. 2723.
4. R.P. Mathur and T. Vasudevan*, Corros*., 38 (1982) 171.
5. F. Zucchi and G. Trabanelli, Proceedings of the 7th European Symposium on Corrosion Inhibitors, Ferrara, 1990, p. 339.
6. E. McCafferty and N. Hackerman, *J. Electrochem. Soc*., 119 (1972) 999.
7. R. Hariharaputhran, A. Subramanian, A.A. Antony, P.M. Sankar, A. Gopalan, T. Vasudevan and I.S Vencatakrishna, *Br. Corros. J*., 33 (1998) 214.
8. E.S. Ivanov, Inhibitors for Metal Corrosion in Acid Media, Metallurgy, Moscow, 1986.
9. Z.A. Foroulis, Proceedings of the 6th European Symposium on Corrosion Inhibitors, Ferrara, 1985, p. 48.
10. Q.J. Slaiman and H.M. Al-Saaty, Proceedings of the 7th European Symposium on Corrosion Inhibitors, Ferrara, 1990, p. 149.
11. I.A. Ammar and F.M. El Khorafi, *Werkstoffe und Korrosion*, 24 (1973) 702.
12. O. Radovici, Proceedings of the 2nd European Symposium on Corrosion Inhibitors, Ferrara, 1965, p. 178.
13. T. Szauer and A. Brandt*, Electrochim. Acta*., 26 (1981) 1209.
14. Mohammed A. Amin, Sayed S. Abd El-Rehim, E.E. F. El-Sherbini and Rady S. Bayoumi, *Electrochim. Acta*., 52 (2007) 3588.
15. B.A. Boukamp, Equivalent Circuit, Princeton Applied Research Corporation, Princeton, N J (1990).

16. S.S. Abd El-Rehim, H.H. Hassan and M.A. Amin, *Mat. Chem. & Phys*., 70 (2001) 64.
17. S.S. Abd El-Rehim, H.H. Hassan and M.A. Amin, *Mat. Chem. & Phys*., 78 (2002) 337.
18. Mohammed A. Amin, *J. Appl. Electrochem*., 36 (2006) 215.
19. S.S. Abdel Rehim, H.H. Hassan and M.A Amin, *Appl. Surf. Sci*., 187 (2002) 279.
20. O.E. Barcia, O.R. Mattos, N. Pebere and B. Tribollet, *J. Electrochem. Soc*., 140 (1993) 2825.
21. C. Deslouis, B. Tribollet, G. Mengoli and M.M. Musiani, *J. Appl. Electrochem*., 18 (1988) 374.
22. H.J.W. Lenderink, M.V.D. Linden. And J.H.W. De Wit, *Electrochim. Acta*., 38 (1993) 1989.
23. B.B. Damaskin, O.A. Petrii and B. Batraktov, Adsorption of Organic Compounds on Electrodes, Plenum Press, New York, 1971.
24. I. Langmuir, *J. Am. Chem. Soc*., 39 (1917) 1848.
25. R. Alberty and R. Silbey, Physical Chemistry, 2nd Edition, Wiley, New York, 1997, p. 845.
26. J. O'M. Bockris and S.U.M. Khan, Surface Electrochemistry: A Molecular Level Approach, Plenum Press, New York, 1993.
27. J.W. Schapinik, M. Oudeman, K.W. Leu and J.N. Helle, *Trans. Farad. Soc*., 56 (1960) 415.
28. A.N. Frumkin, *Z. Phys. Chem*., 116 (1925) 466.
29. O. Ikeda, H. Jimbo and H. Tamura, *J. Electroanal. Chem*., 137 (1982) 127.
30. J. Hill de Boer, The Dynamical Character of Adsorption, 2nd Edition, Clarendon Press, Oxford, UK, 19683
31. H. Dhar, B. Conway and K. Joshi, *Electrochim. Acta*, 18 (1973) 789.
32. E. Kamis, I. Mellucci, R.M. Lantanision and E.S.H. El-Ashry, *Corros.*, 47 (1991) 677.
33. D. Do, Adsorption Analysis: Equilibria and Kinetics, Imperial College Press, 1998, pp. 10-60.
34. F.M. Donahue and K. Nobe*, J. Electrochem. Soc*., 112 (1965) 886.
35. W. Durnie, R.D. Marco, A. Jefferson, B. Kinsella, *J. Electrochem. Soc*., 146 (1999) 1751.
36. S. Martinez and I. Stern, *Appl. Surf. Sci*., 199 (2002) 83.
37. S. Martinez, Mater. *Chem& Phys*., 77 (2003) 97.
38. M.J. Lampinen and M. Fomino, *J. Electrochem. Soc*., 140 (1993) 3537.
39. J. O'M. Bockris, A.K.N. Reddy, Modern Electrochemistry, Vol. 2, Plenum Press, New York, 1977, p. 1267.
40. T. Szauer, A. Brandt, *Electrochim. Acta*, 26 (1981) 943.
41. E. F. El Sherbini*, Mat. Chem. & Phys*., 60 (1999) 286.
42. J.M. Bastidas, J. De Dambornea, A.J. Vazquez, *J. Appl. Electrochem*., 27 (1997) 345.
43. F. Mansfeld, Corrosion Mechanism, p. 119. Marcel Dekkar, New York (1987).